

in fibres fourteen years before this was confirmed in a crystal; the behaviours of starch, cellulose, as well as connective tissue and other gel-forming polysaccharides have been rationalized exclusively from fibre diffraction studies; the structures of DNA and RNA single, double, triple and quadruple helices were defined from fibre analyses up to a quarter of a century before analogous structures were disclosed in single crystals.

Fibre diffraction analysis has many past achievements to be proud of and many future triumphs to anticipate.

## References

- [1] Wang, A.H.-J., Quigley, G.J., Kolpak, F.J., Crawford, J.L., van Broom, J.H., van der Marel, G. and Rich, A., *Nature* (1979) **281**, 680.
- [2] Arnott, S., Chandrasekaran, R., Birdsall, D.L., Leslie, A.G.W. and Ratliff, R.L., *Nature* (1980) **287**, 561.
- [3] Dickerson, R.E., *Meth. Enzymol.* (1992) **211**, 67.
- [4] Arnott, S., Chandrasekaran, R., Millane, R.P. and Park, H.-S., *J. Mol. Biol* (1986), **188**, 631.
- [5] Rich, A. and Crick, F.H.C., *J. Mol. Biol* (1961) **3**, 483.
- [6] Fraser, R.D.B., MacRae, T.P. and Suzuki, E., *J. Mol. Biol* (1979) **129**, 463.
- [7] Okuyama, K., Arnott, S., Takayanagi, M. and Kakudo, M., *J. Mol. Biol.* (1981) **152**, 427.
- [8] Bella, J., Eaton, M., Brodsky, B. and Berman, H.M., *Science* (1994) **266**, 75.
- [9] Chandrasekaran, R., in *Adv. in Carbohydrate Chemistry and Biochemistry* (1997) **52**, 311.
- [10] Balazs, E.A., *Fed. Proc* (1966) **25**, 1817.
- [11] Arnott, S. and Wonacott, A.J., *J. Mol. Biol* (1966) **21**, 371.
- [12] Arnott, S., Mitra, A.K. and Raganathan, *J. Mol. Biol* (1983) **169**, 861.
- [13] Crick, F.H.C. and Watson, J.D., *Peoc. R. Soc. (London) Ser. A* (1954) **223**, 80.
- [14] Arnott, S. in *Bull. Inst. Phys. and Phys. Soc* (1964), 169-178.
- [15] Arnott, S., Wilkins, M.H.F., Hamilton, L.D. and Langridge R., *J. Mol. Biol* (1965) **27**, 391.
- [16] Arnott, S., in *Oxford Handbook of Nucleic Acid Structure* (1998), 1-36.

## X-Ray Studies on Biological Fibres

A. Miller, J.P. Orgel and T.J. Wess

University of Stirling

The most important scientific paper of the second half of the twentieth century was a report of X-ray fibre diffraction studies on DNA. Biological fibres have well developed crystallinity in the direction of the fibre axis, but are not so well ordered in the directions normal to the fibre axis. This simple one-dimensional order meant that fibres allowed the first recognition of the secondary structure of proteins - the alpha helix, beta sheet, coiled-coil alpha helix and collagen helix - as well as the double helix of DNA, long before X-ray crystallography yielded the full three-dimensional structures of biological macromolecules and complexes. In addition X-ray fibre diffraction studies gave information about the molecular packing in the native biological fibres of muscle, tendons and the cytoskeleton and it is this window into structural molecular biology which is the subject of this note.

Advances in the technology of X-ray fibre diffraction have always been the basis of its value. Small angle cameras with good resolution between the undeflected beam and the scattered beam closest to it, good reciprocal spatial resolution throughout the scattered pattern, intense X-ray sources of high spectral brilliance and efficient and effective X-ray detectors have all played their part. So we will start by discussing some aspects of synchrotron radiation which are undergoing developments which will be relevant to fibre work - as well as to macromolecular crystallography - in the near future. We then summarise our recent work on the molecular packing of Type I collagen in tendons and comment on recently published claims about features in the X-ray diffraction patterns from the alpha-keratin of hair and their relationship to breast cancer.

## Synchrotron Radiation

Third generation synchrotron sources such as the ESRF at Grenoble introduced the feature of flexibility of insertion devices which could be custom designed for specific scientific applications. In second generation synchrotrons the flexibility lay mainly in the design of the beam lines. Hence at ESRF, once the machine energy was decided as 6

GeV and the emittance of the electron beam set as  $7 \times 10^{-9}$  nm.rad, the task remained to survey the proposals of the scientist users and to build a set of beam-lines on Insertion Devices (IDs) tailored within technically feasible limits for defined areas of science. A balance was struck between beam-lines which would allow a high volume of new science to be done and other beam-lines which served smaller groups of scientists working at extremes of technology such as in high X-ray energy, high pressure studies or recondite techniques such as Mossbauer scattering.

Since the ESRF was founded in 1986 and opened in 1993 as planned, there have been many advances in machine design allowing lower emittance electron beams and improvements in ID design which will affect the choice of energy of the new generation of synchrotron sources and in particular allow lower energy (and thus cheaper) machines to produce X-rays of high brilliance in the energy range up to 20KeV. The main parameter in IDs which can be lowered is the inter-magnet gap across the electron beam. When ESRF started this was set prudently at a minimum of 20 mm. Now ESRF can run with a gap of 8 mm. The lower gap means that with a fixed electron beam energy in the machine and fixed magnetic field in the ID the energy of the emitted X-rays is higher than with a wider gap. At a meeting held in Daresbury in May 1999 (Chair - M.W. Poole) there were reports of experiences with smaller gaps at synchrotron sources world wide. It was concluded that to achieve gaps of lower than 5 mm it was necessary to have the magnets of the ID *in vacuo* and then gaps of 2 mm could be countenanced. However, operation *in vacuo* brings additional technical problems and risks. A. Ropert concluded that *in vacuo* was necessary for a gap less than 5 mm and Marcouille working with calculations done for SOLEIL concluded that 25 KeV X-rays can be produced with a 1.5 m long *in vacuo* device with a 4 mm gap from a 2.5 GeV machine. Another factor emerging from recent experience of building undulators is that high harmonics - around the 11th - can be used with tolerable loss in brilliance. These considerations are central in discussions about machine energy, design of IDs and of beam-lines for fibre diffraction at the planned UK-Wellcome-French synchrotron.

### Molecular Packing in Collagen

We have produced a model-independent solution to

the phase problem for a native biological fibre, Type I collagen in tendon, using Multiple Isomorphous Addition (Orgel, Wess and Miller, 2000). This technique has been used previously to produce an electron density projection on to the fibre axis (Bradshaw *et al.* 1989) where the first 52 meridional orders of diffraction in the X-ray fibre pattern were used.

Using synchrotron radiation at Daresbury Laboratory, UK (Beamlines 7.2 and 2.1) and at the European Synchrotron Radiation Facility, Grenoble, France (Beamline ID2) we have recorded over 140 meridional orders of diffraction. Of these, 124 orders from native tendons and tendons stained isomorphously with gold chloride and potassium iodide have been utilised to produce the electron density profile in Figure 1. The resolution of this electron density projection is more than two times higher than that produced previously.

The new electron density map to 0.54 nm resolution reveals that the collagen molecule *in vivo* is 4.54 D long, where each staggered segment (D) is 66.7 nm and corresponds to 234.2 amino acids. It also shows that the C-terminal telopeptide is in a folded conformation and the N-terminal telopeptide is axially contracted compared with the conformation in the collagen triple helix.

However, the key findings of this new high resolution study pertain to the intermolecular crosslinks which are essential to maintain the structural integrity of the collagen fibrils in native healthy tissue (Eyre *et al.*, 1984). The telopeptides are those formed by amino acid sequences at the end of the molecule which do not have the regular Gly-X-Y feature and so cannot coil into the collagen triple helical conformation.

There are 25 amino acids in the alpha 1 C-terminal chain and our electron density projection presents strong evidence that there is a hairpin turn at proline 13 and glutamine 14. This would bring tyrosine residue 24 into axial alignment with tyrosine 4 and bring lysine 17 into a favourable position to form a lysine-hydroxylysine crosslink with hydroxylysine 87 thus helping to stabilise the fibril structure (Figure 2).

This study provides for the first time model-independent information about the all important intermolecular crosslinks.

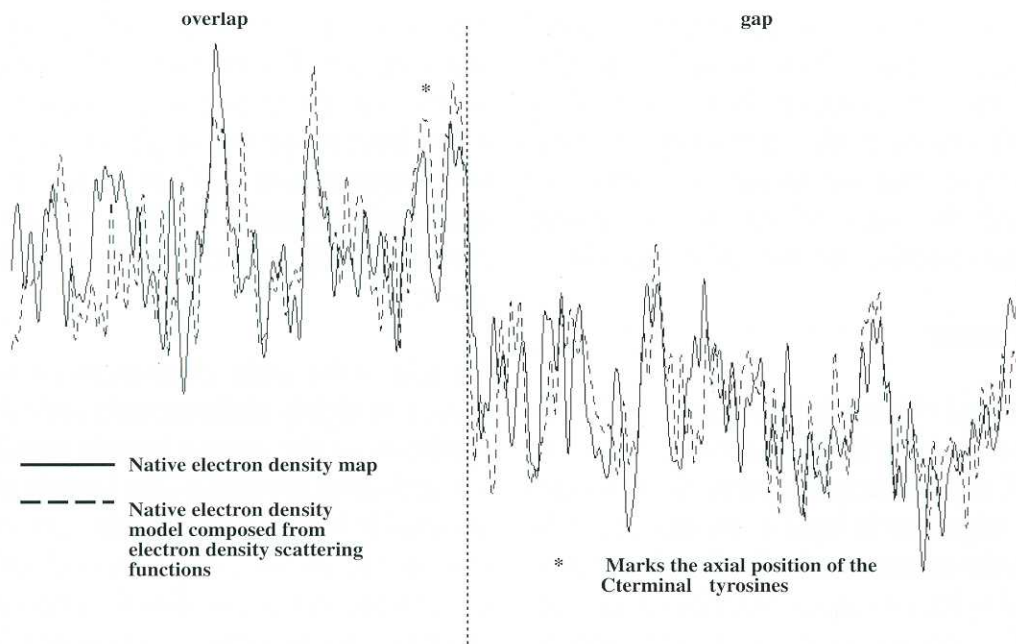


**Figure 1:** 1-Dimensional Electron density profile of type I collagen. The resolution of the electron density projection (or 1D electron density map) is 0.54 nm. Overlaid is an electron density model composed from residue scattering factors and the amino acid sequence. The residue spacing in the model was constant, the N-telopeptide contracted by 85%, and the C-telopeptide was folded at residues 13 and 14.

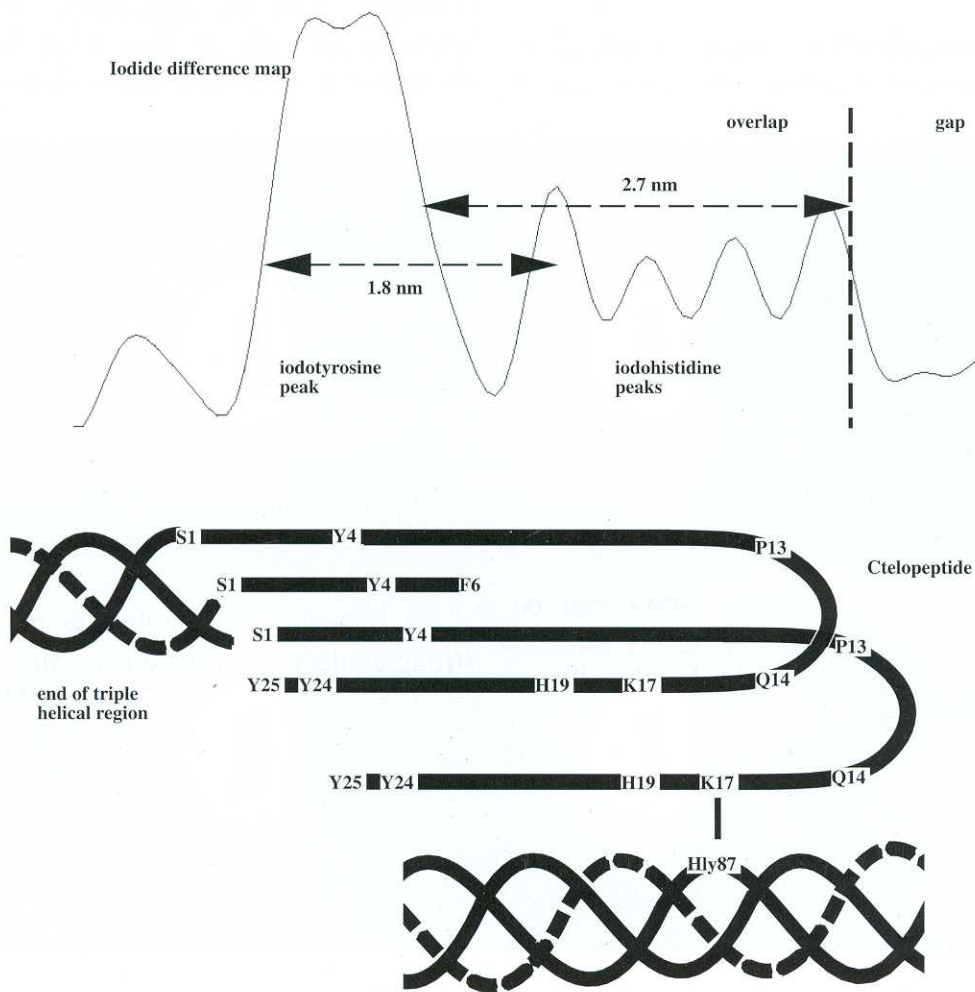


**Figure 2:** Conformation of the C-telopeptide restricted by heavy atom positions. An expanded view of the C-terminal telopeptide region shows a conformation that corresponds well with the difference density data.

We are now carrying out a similar project to obtain a model-independent three-dimensional electron density distribution of collagen in native tendon. Obviously the resolution in the electron density map will be anisotropic, but we expect to locate the telopeptides and the sites of the intermolecular crosslinks and to visualise the molecular packing.

### Keratin and Cancer

In an article entitled "Using hair to screen for breast cancer" James *et al.* (1999) reported that the occurrence in X-ray diffraction patterns from female human hair of rings due to lipid scattering could be correlated with the occurrence in the female subjects of a gene linked to breast cancer. Needless to say this report attracted widespread comment in the media. We wish to criticise the conclusion drawn by James *et al.* on several grounds. First the number of samples used in the study was far too small to justify the conclusion. Secondly, there was no discussion of other factors such as the effect on hair of state of health of the subjects, washing detergents, anti-cancer drug therapy etc.

However, the most important criticism is that there was no reference to earlier work on the occurrence of

lipid rings in the X-ray diffraction patterns from alpha keratin (Fraser *et al.* 1963). This is particularly significant since Fraser *et al.* presented evidence for a mechanism for the origin of the lipid rings. The best interpretation that can be put on this is that the apparently dramatic findings of James *et al.* were published in ignorance of a highly relevant previous study.

Keratin is the main component of human hair and occurs in highly differentiated cells dedicated to the synthesis of the protein keratin within the cells. As keratinisation progresses the keratin fills the cell and eventually kills it. The hair and skin on the surface of humans are mostly composed of dead cells. Fraser *et al.* carried out a combined X-ray diffraction and electron microscopy examination of hair as it develops from the follicle just under the skin to the fully keratinised tissue. They found that in the early stages of keratinisation there were no lipid rings in the X-ray diffraction patterns from hair at that point. As keratinisation progressed away from the follicle the lipid rings appeared. Electron microscopy showed that the appearance of these rings could be correlated with the appearance of crystallites of lipids in the cells as they were deformed by the development of keratin fibres (Fraser *et al.*, 1963).

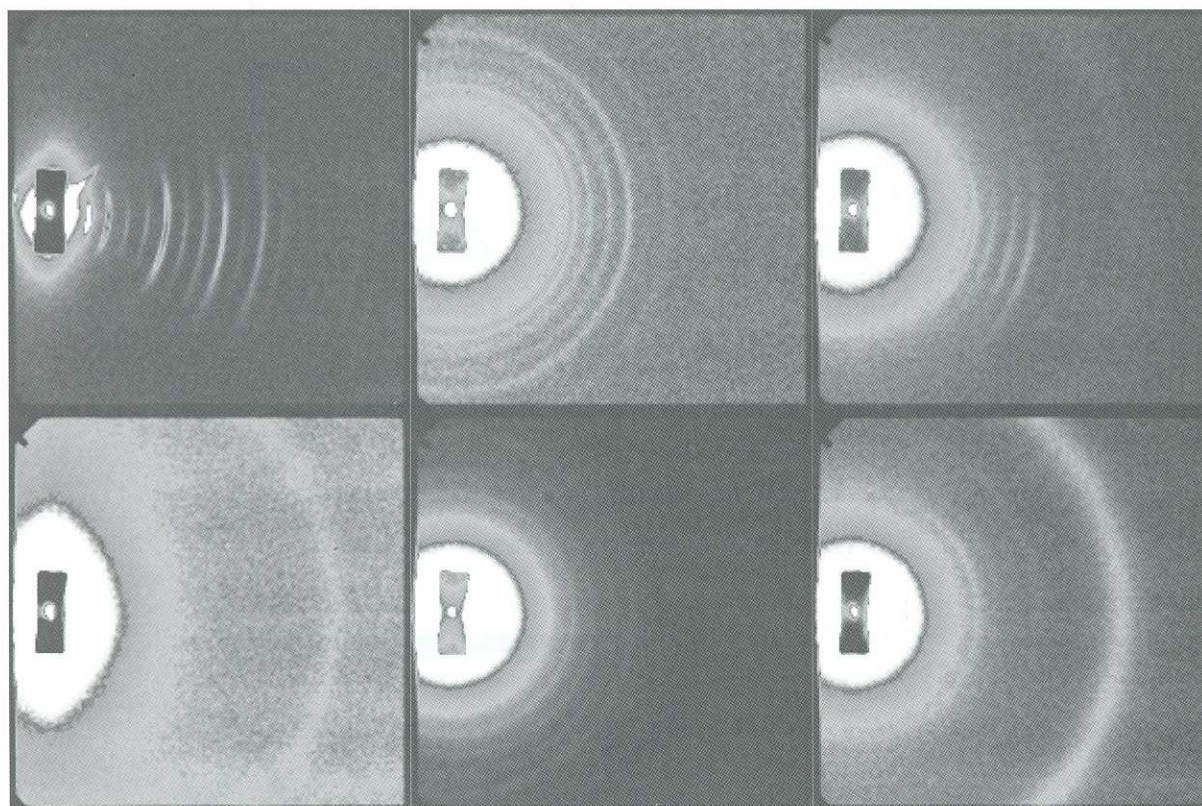


**Figure 3:** X-ray diffraction image of dry collagen samples containing diffuse isotropic diffraction ring from lipids. The samples are historic parchment sample from the 17th century provided by the Danish National Archive. Unpublished results indicate that lipid crystallisation is related to ageing of the parchment samples. The lipid ring corresponds to a periodicity of 4.5nm. Data were collected using a 6 metre camera on beamline 2.1 of the Daresbury synchrotron.

## Unravelling Starch Granule Structure with Small Angle Scattering

A.M. Donald, P. A. Perry and T.A. Waigh

Cavendish Laboratory, Madingley Road, Cambridge CB3 0HE, UK

The lipid crystallites in the electron micrographs showed bands spaced some 4.7 nm apart and this spacing corresponded with that observed in the lipid rings in the X-ray diffraction patterns. The crystallites seemed to be formed by rearrangement of the membranes of the cell mitochondria.

On the basis of what is in the scientific literature at present there is no reason to believe that the variation in appearance of lipid rings in X-ray diffraction patterns from hair is not due to the degree of keratinisation in the hair cells and is unrelated to cancer. Indeed, Wilk, James and Amemiya (1995) reported that "oil" is an integral component of all samples of human scalp hair.

It is worth pointing out that X-ray diffraction patterns from other biological fibres such as collagen often contain rings that index on the lipid spacing (Figure 3).

An alternative explanation for the presence of the isotropic diffraction ring is possible due to its close proximity with the 4.5 nm equatorial diffraction peak. The 4.5 nm reflection corresponds to the cylindrical transform of an  $\alpha$ -helical bundle. It is possible that keratin samples exhibiting diffuse scatter contain microfibrils that are randomly orientated and have a low packing density. These would exhibit negligible intermolecular interference and produce arcs of diffuse scatter that would roughly correspond to those observed by James *et al.* Samples containing disordered arrays of microfibrils suggest that the biogenesis of the hair was disrupted in some way. Perhaps it is possible that radiation and chemotherapy would cause such disruption.

### References

- [1] Fraser, R.D.B., MacRae, T.P., Rogers, G.E. and Filshie, B.K., *J. Mol. Biol.* (1963) **7**, 90-91.
- [2] James, V., Kearsley, J., Irving, T., Amemiya, Y. and Cookson, D., *Nature* (1999) **398**, 33-34.
- [3] Wilk, K.E., James, V.J. and Amemiya, Y., *Biochim. Biophys. Acta.* (1995) **1245**, 392-396.
- [4] Eyre, D.R., Paz, M.A. and Gallop, P. M., *Ann. Rev. Biochem.* (1984) **53**, 717-748.
- [5] Bradshaw, J.P., Miller, A. and Wess, T.J., *J. Mol. Biol.* (1989) **205**, 685-694.
- [6] Orgel, J.P., Wess, T. J. and Miller, A., *Structure* (2000) **8**, 134-141.

### Introduction

Starch is a natural source of polymers of huge commercial importance both for food and industrial use (as in paper-coatings). As knowledge of starch biochemistry improves, as does the ability of plant scientists to produce novel starches (not necessarily, but possibly, via genetic modification routes), it is important to be able to understand the impact of such changes on structure and subsequent processing. In order to explore the hierarchical internal structure of the native granule, and how it breaks down during processing ('cooking'), small angle scattering of both neutrons and X-rays have been used in a complementary approach.

The native starch granule contains two main polysaccharides, amylopectin and amylose. Amylopectin is highly branched and is the component which crystallises. It does so via double helix formation of the side chain branches which then aggregate to form the crystals. Amylose, on the other hand, is an essentially linear polysaccharide. The proportions of these two polysaccharides, and the molecular weights of the chains (which are always very high, running to many millions in the case of amylopectin) are species-dependent. However, in wild-type species, there is usually approximately 70% amylopectin and 30% amylose. Most starches contain minor amounts of other components including lipids and proteins, but they will not be further discussed here.

### Experimental Methods

Various different commercially available starches have been used. Each starch has been made up as a slurry at 40-45 w/w% in the appropriate solvent (water, which may have included D<sub>2</sub>O for SANS experiments, or glycerol). The starch slurry was sealed in a cell which was made of aluminium for SAXS experiments, and quartz for SANS. Experiments were carried out on beamline 8.2 at the